

Fig. 1

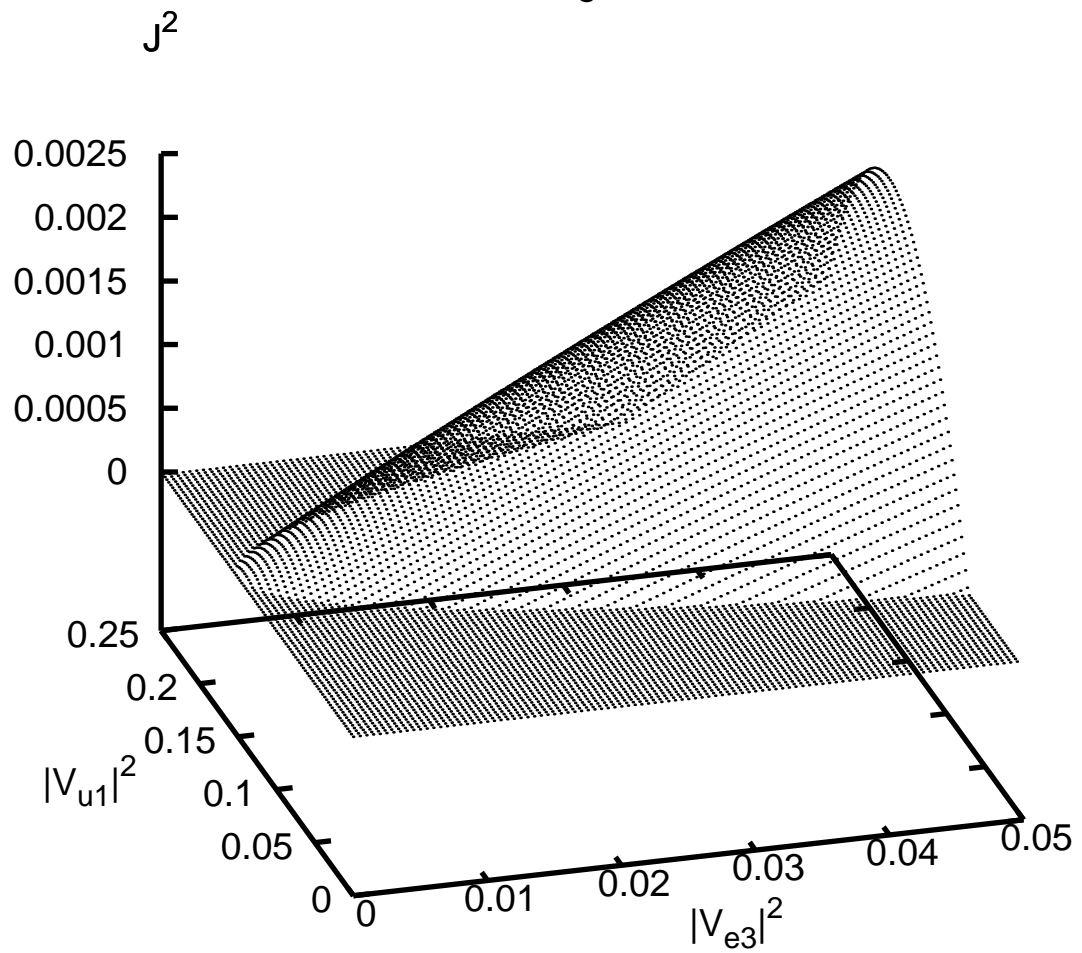


Table I

\mathcal{V}_{e2}^2	\mathcal{V}_{e3}^2	\mathcal{V}_{e3}^2	$1; 2; \mathcal{V}_{12}^2$	$\cos(\theta)$	$\cos(\theta)_c$	$\cos(\theta)_+$
0.30 (10)	0.50 (10)	0.03 (10)	$1 = 1:0$ (10)	-0.257	0.056	0.387
			$2 = 2:3$ (10)	-0.300	0.111	0.457
			$\mathcal{V}_{12}^2 = 0:15$ (10)	-0.708	-0.132	0.442
0.30 (5)	0.50 (5)	0.01 (5)	$1 = 1:0$ (5)	-0.224	0.033	0.294
			$2 = 2:3$ (5)	-0.285	0.042	0.329
			$\mathcal{V}_{12}^2 = 0:15$ (5)	-0.569	-0.076	0.414
0.30 (5)	0.50 (5)	0.01 (20)	$1 = 1:0$ (5)	-0.247	0.033	0.310
			$2 = 2:3$ (5)	-0.303	0.042	0.343
			$\mathcal{V}_{12}^2 = 0:15$ (5)	-0.607	0.076	0.457
0.30 (5)	0.50 (5)	0.01 (5)	$1 = 1:0$ (10)	-0.306	0.033	0.391
			$2 = 2:3$ (10)	-0.404	0.042	0.440
			$\mathcal{V}_{12}^2 = 0:15$ (10)	-0.747	-0.076	0.599
0.30 (5)	0.50 (5)	0.015 (5)	$1 = 1:0$ (5)	-0.170	0.040	0.255
			$2 = 2:3$ (5)	-0.190	0.065	0.300
			$\mathcal{V}_{12}^2 = 0:15$ (5)	-0.493	-0.093	0.306
0.30 (5)	0.50 (5)	0.005 (5)	$1 = 1:0$ (5)	-0.339	0.023	0.392
			$2 = 2:3$ (5)	-0.429	0.007	0.412
			$\mathcal{V}_{12}^2 = 0:15$ (5)	-0.756	-0.054	0.642
0.30 (5)	0.50 (2)	0.001 (25)	$1 = 1:0$ (5)	-0.529	0.010	0.555
			$2 = 2:3$ (5)	-1.0	-0.081	0.885
			$\mathcal{V}_{12}^2 = 0:15$ (5)	-1.0	-0.024	1.0
0.30 (2)	0.50 (5)	0.001 (25)	$1 = 1:0$ (5)	-0.879	0.010	0.901
			$2 = 2:3$ (5)	-0.796	-0.081	0.552
			$\mathcal{V}_{12}^2 = 0:15$ (5)	-1.0	-0.024	1.0

Values of $\cos(\theta)$ for different combinations of parameters: $\cos(\theta)_c$ is obtained from the central values of the parameters while $\cos(\theta)_-$ and $\cos(\theta)_+$ are the extremum values allowed by the uncertainties (shown in percent, in parentheses next to each parameter).

Fig. 2

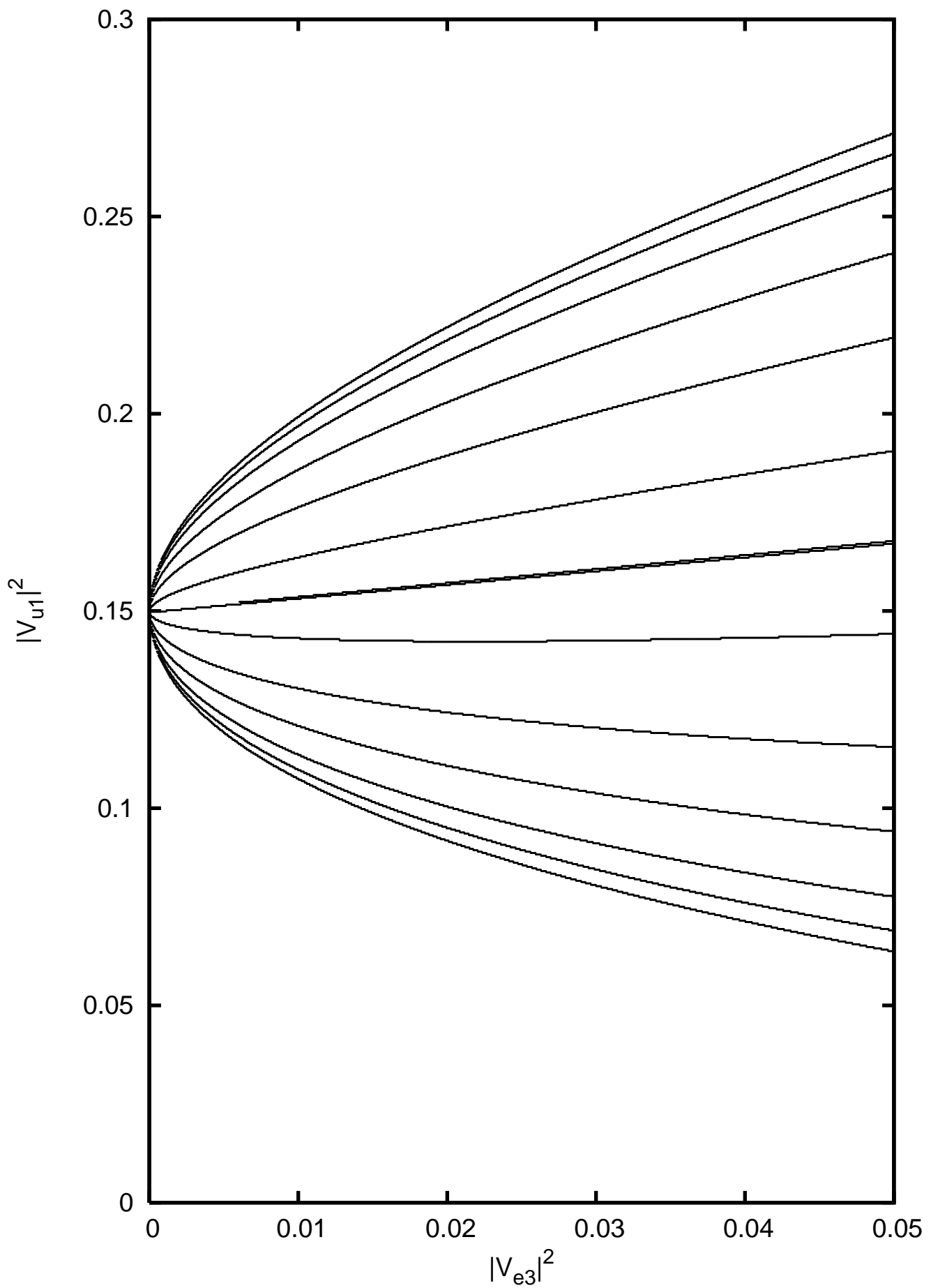


Table II

\mathcal{V}_{e2}	\mathcal{V}_{31}	\mathcal{V}_{e3}	$\mathcal{V}_{12}; \mathcal{V}_{13}$	$\cos(\theta)$	$\cos(\theta)_c$	$\cos(\theta)_+$
0.30 (5)	0.40 (5)	0.01 (5)	$\mathcal{V}_{12} = 0.68$ (5)	-0.204	0.025	0.247
			$\mathcal{V}_{12} = 2.2$ (5)	-0.294	-0.034	0.195
			$\mathcal{V}_{12} = 0.18$ (5)	-0.615	-0.076	0.458
0.30 (10)	0.40 (5)	0.01 (5)	$\mathcal{V}_{12} = 0.68$ (5)	-0.213	0.025	0.254
			$\mathcal{V}_{12} = 2.2$ (5)	-0.446	-0.034	0.330
			$\mathcal{V}_{12} = 0.18$ (5)	-0.813	-0.076	0.665
0.30 (5)	0.40 (10)	0.01 (5)	$\mathcal{V}_{12} = 0.68$ (5)	-0.349	0.025	0.383
			$\mathcal{V}_{12} = 2.2$ (5)	-0.310	-0.034	0.199
			$\mathcal{V}_{12} = 0.18$ (5)	-0.765	-0.076	0.582
0.30 (5)	0.40 (5)	0.01 (10)	$\mathcal{V}_{12} = 0.68$ (5)	-0.212	0.025	0.250
			$\mathcal{V}_{12} = 2.2$ (5)	-0.306	-0.034	0.196
			$\mathcal{V}_{12} = 0.18$ (5)	-0.628	-0.076	0.471
0.25 (2)	0.55 (2)	0.01 (2)	$\mathcal{V}_{12} = 0.8$ (2)	0.551	0.650	0.760
			$\mathcal{V}_{12} = 3.85$ (2)	0.541	0.652	0.770
			$\mathcal{V}_{12} = 0.145$ (2)	0.481	0.663	0.856
0.25 (2)	0.55 (2)	0.01 (25)	$\mathcal{V}_{12} = 0.8$ (2)	0.553	0.650	0.854
			$\mathcal{V}_{12} = 3.85$ (2)	0.543	0.652	0.852
			$\mathcal{V}_{12} = 0.145$ (2)	0.482	0.663	0.993

Values of $\cos(\theta)$ for different combinations of parameters: $\cos(\theta)_c$ is obtained from the central values of the parameters while $\cos(\theta)_-$ and $\cos(\theta)_+$ are the extremum values allowed by the uncertainties (shown in percent, in parentheses next to each parameter).

Table III

\mathcal{V}_{e2}^2	\mathcal{V}_{e3}^2	\mathcal{V}_{e3}^2	\mathcal{V}_{12}^2 \mathcal{V}_{14}^2	R_e	R_e
0.3	0.5	0.01	0.11 0.20	0.94 1.04	0.95 1.06
0.3	0.5	0.005	0.12 0.18	0.96 1.03	0.96 1.03
0.35	0.5	0.01	0.13 0.23	0.94 1.03	0.96 1.05
0.35	0.55	0.01	0.12 0.21	0.88 0.95	0.91 0.99
0.35	0.4	0.01	0.17 0.26	1.05 1.14	1.14 1.22
0.35	0.6	0.01	0.10 0.19	0.80 0.86	0.86 0.95
0.25	0.6	0.01	0.063 0.145	0.81 0.90	0.86 1.00
0.3	0.6	0.01	0.081 0.17	0.81 0.88	0.86 0.98

Different values of R_e and R_e for different combinations of 4 independent \mathcal{V}_{ij}^2 . \mathcal{V}_{12}^2 and \mathcal{V}_{14}^2 span the range allowed by unitarity and positivity of \mathcal{U}^2 ; these extremum values of \mathcal{V}_{12}^2 correspond to vanishingly small CP violation.

Table IV

\mathcal{V}_{e2}^f	\mathcal{V}_{3f}	\mathcal{V}_{e3}^f	R_e	$\cos(\theta)$	$\cos(\theta)_c$	$\cos(\theta)_+$
0.30 (1)	0.50 (1)	0.01 (1)	1.00 (1)	-0.183	0.118	0.463
0.30 (10)	0.5 (1)	0.01 (25)	1.00 (1)	-0.265	0.118	0.567
0.30 (2)	0.50 (2)	0.01 (2)	1.00 (2)	-0.463	0.118	0.891
0.30 (1)	0.50 (1)	0.005 (1)	1.00 (1)	-0.332	0.082	0.550
0.30 (2)	0.50 (2)	0.005 (2)	1.00 (2)	-0.718	0.082	1.0
0.30 (5)	0.50 (1)	0.005 (10)	1.00 (1)	-0.373	0.082	0.600
0.30 (1)	0.60 (1)	0.01 (1)	0.84 (1)	-0.605	-0.211	0.257
0.30 (2)	0.60 (2)	0.01 (2)	0.84 (2)	-0.949	-0.211	0.867
0.30 (5)	0.60 (1)	0.01 (10)	0.84 (1)	-0.653	-0.211	0.348
0.35 (1)	0.45 (1)	0.01 (1)	1.03 (1)	-0.769	-0.485	-0.186
0.35 (2)	0.45 (1)	0.01 (2)	1.03 (1)	-0.792	-0.485	-0.181
0.35 (10)	0.45 (1)	0.01 (10)	1.03 (1)	-0.931	-0.485	-0.121
0.35 (10)	0.45 (2)	0.01 (10)	1.03 (2)	-0.936	-0.485	+0.160
0.24 (2)	0.40 (2)	0.01 (2)	1.06 (2)	-0.476	-0.141	0.205
0.24 (10)	0.40 (2)	0.01 (25)	1.06 (2)	-0.679	-0.141	0.290
0.24 (2)	0.40 (2)	0.01 (2)	1.13 (2)	0.446	0.845	1.0
0.24 (10)	0.40 (1)	0.01 (25)	1.13 (1)	0.579	0.845	1.0
0.24 (2)	0.40 (2)	0.01 (2)	1.13 (5)	-0.076	0.845	1.0
0.25 (1)	0.55 (1)	0.01 (1)	0.94 (1)	-0.165	0.135	0.475
0.25 (10)	0.55 (1)	0.01 (25)	0.94 (1)	-0.244	0.135	0.627
0.25 (2)	0.55 (2)	0.01 (2)	0.94 (2)	-0.440	0.135	0.874
0.25 (5)	0.55 (2)	0.01 (10)	0.94 (2)	-0.46	0.135	0.950

Values of $\cos(\theta)$ for different combinations of parameters: $\cos(\theta)_c$ is obtained from the central values of the parameters while $\cos(\theta)_-$ and $\cos(\theta)_+$ are the extremum values allowed by the uncertainties (shown in percent, in parentheses next to each parameter).

Table V

\mathcal{Y}_{e2}	\mathcal{Y}_{e3}	\mathcal{Y}_{e3}	$\tau_1 = \tau = \tau$	$\cos(\text{eff:})$	$\cos(\text{eff:})_c$	$\cos(\text{eff:})_+$
0.30 (5)	0.50 (5)	0.01 (5)	0.7 (5)	0.377	0.628	0.920
0.30 (5)	0.50 (5)	0.01 (10)	0.7 (5)	0.378	0.628	0.940
0.30 (5)	0.50 (5)	0.01 (5)	0.7 (10)	0.303	0.628	1.0
0.30 (5)	0.50 (5)	0.01 (25)	0.7 (5)	0.380	0.628	1.0
0.30 (5)	0.50 (5)	0.01 (5)	1.3 (5)	-0.685	-0.407	-0.161
0.30 (5)	0.50 (5)	0.01 (5)	1.3 (10)	-0.765	-0.407	-0.072
0.30 (5)	0.50 (5)	0.01 (5)	1.8 (10)	-1.0	-0.931	-0.598
0.25 (5)	0.60 (5)	0.01 (5)	1.8 (5)	-0.522	-0.263	-0.013
0.25 (5)	0.60 (5)	0.01 (5)	3.0 (10)	-1.0	-0.920	-0.624
0.25 (5)	0.60 (5)	0.005 (5)	2.5 (10)	-1.0	-0.971	-0.544

Values of $\cos(\text{eff:})$ for different combinations of parameters in a non-radiative decay scenario: $\cos(\text{eff:})_c$ is obtained from the central values of the parameters while $\cos(\text{eff:})$ and $\cos(\text{eff:})_+$ are the extremum values allowed by the uncertainties (shown in percent, in parentheses next to each parameter).

Canonical constraints on leptonic CP violation using UHCR neutrino fluxes

K. R. S. Balaji^{1,2,3}, Gilles Couture², Cherif Hamzaoui²¹ Department of Physics, McGill University, Montreal, QC, Canada H3A 2T8² Department des Sciences de la Terre et de l'Atmosphère, Université du Québec à Montréal,

CP 8888, succ. centre-ville, Montréal, QC, Canada H3C 3P8 and

³ Physique des Particules, Université de Montréal CP 6128,

succ. centre-ville, Montréal, QC, Canada H3C 3J7

It is shown that one can in principle constrain the CP-violating parameter from measurements of four independent y_{ij}^2 's, or three y_{ij}^2 and a ratio of two of them, in the leptonic sector. To quantify our approach, using unitarity, we derive simple expressions in terms of four independent y_{ij}^2 's for \cos , and an expression for \sin^2 from J^2 . Thus, depending on the values for y_{ij}^2 and their accuracy, we can set meaningful limits on y_{ij}^2 . To illustrate numerically, if y_{12}^2 is close to 0.1 with a 10% precision, and if y_{e3}^2 is larger than 0.005 and for values of y_{e2}^2 and y_{34}^2 that stay within 0.1 of the current experimental data leads to a bound: $= 2 \pi y_{12}^2$. Alternatively, a certain combination of parameters with values of y_{e3}^2 larger than 0.01 leads to a closed bound of $73 \pi y_{12}^2 \approx 103$. In general, we find that over most of the parameter space, y_{12}^2 is least sensitive to y_{e3}^2 . With just three independent measurements (solar, atmospheric and reactor), it is impossible to set limits on the CP phase. In this respect, we study the use of ultra high energy cosmic ray (UHCR) neutrino fluxes as the additional fourth information. We find that within the SM, neutrino fluxes of all three flavours will be very similar but that pushing current neutrino data to their extreme values still allowed, ratios of cosmic neutrino fluxes can differ by up to 20%; such large discrepancies could imply negligibly small CP-violation. We also study a non radiative neutrino decay model and find that the neutrino fluxes can differ by a factor of up to 3 within this model and that an accuracy of 10% on the neutrino fluxes is sufficient to set interesting limits on y_{12}^2 .

PACS numbers: 98.80.Cq.

I. INTRODUCTION

One of the significant achievements of particle physics has been our better understanding of the leptonic flavor mixings. Following some very detailed and pains-taking measurements the neutrino anomaly has now been confirmed; both in the solar and atmospheric sector [1]. An immediate conclusion is the existence of new physics beyond standard model and to introduce a small neutrino mass. Such an extension leads to the notion of neutrino oscillation [2] similar in spirit to quark sector. A genuine three flavor analysis, allows for a solution space consisting of two mass-squared differences and three angles. The solution amounts to finding the allowed parameter space for the solar mass angle, and the atmospheric mixing angle along with a strongly constrained reactor angle. Phenomenologically, best fit values and allowed range for these three mixing parameters dictates a pattern that is almost being negligible (reactor) to moderate (solar) to maximal (atmospheric). For a review on the analysis, we refer to [3].

Similar to the quark sector, one can have CP violation in the leptonic sector due to massive neutrinos. The CP violation can come due to both Dirac and Majorana phases in the mixing matrix depending on the nature of the neutrinos. As a pertinent question, how to measure CP violation in neutrino oscillations has attracted a lot of attention in the past [4] and no doubt, the search for leptonic CP violation will be one of the main goals of experimental particle physics in the years to come. Given

the strong reactor constraints [5] it is very difficult for current neutrino oscillation experiments to measure CP-violation. Nonetheless, as a proposal, a measurement is possible by one searching for differences between neutrino and anti-neutrino survival in a long-baseline experiment and measuring the spectrum [6].

In the present analysis, we want to explore the possibility of extracting information on CP violation in the leptonic sector without performing a direct CP violation experiment. Clearly, such an experiment will have to be done eventually but in the near future, it might be easier to measure individual lepton mixing matrix elements (y_{ij}^2). Thus, it becomes interesting to see how information about these can be translated into information about CP violation in the leptonic sector and what level of precision will be required on the y_{ij}^2 's to set interesting constraints on y_{12}^2 .

In the next section, we will contrast two parameterizations that represent leptonic mixing; the usual PMNS parameterization (in terms of mixing angles and phases) [7] and another one constructed purely as moduli elements, where CP violation is not explicit but still present. Following this, we will derive expressions that allow one to extract information on CP violation from measurements of four y_{ij}^2 's or combinations of them. These relations are used to calculate the precision on the measurements of the y_{ij}^2 's required in order to set constraints on y_{12}^2 . We will then consider the use of UHCR neutrino fluxes to obtain the fourth y_{ij}^2 needed to set constraints on y_{12}^2 . We also derive general relations about their fluxes and estimate the precision required in

We can also calculate what value of \mathcal{Y}_1^2 will maximize J^2 such that $\mathcal{Y}_1^2 = J_{\max}^2$. Differentiating J^2 with respect to \mathcal{Y}_1^2 and retaining only first order in \mathcal{Y}_{e3}^2 , one then recovers the first two terms of (2.7). This is consistent since maximizing J^2 requires $\sin^2 = 1$. One observes here that a value of \mathcal{Y}_1^2 larger than $\mathcal{Y}_1^2 = J_{\max}^2$ requires to be in the first or in the fourth quadrant. This simple point does not require particularly precise data and could already be useful information for model builders.

In the standard V_{PMNS} basis, J^2 is given by [11]

$$J^2 = \sin^2(12) \cos^2(12) \sin^2(23) \cos^2(23) \sin^2(13) \cos^2(13) \cos^2(13) \sin^2(1) \quad (2.13)$$

Clearly, whether in the V_{PMNS} or in our current basis, J^2 is the same physical observable and we can compare the two expressions for this parameter. Using the relations between the V_{ij} and $\sin(\mathcal{Y}_{ij})$, we express J^2 in terms of $\sin^2(1)$ and three of our \mathcal{Y}_{ij}^2 :

$$J^2 = \frac{1}{(1 - \mathcal{Y}_{e3}^2)^2} \mathcal{Y}_{e2}^2 \mathcal{Y}_3^2 \mathcal{Y}_{e3}^2 (1 - \mathcal{Y}_{e3}^2 - \mathcal{Y}_{e2}^2) (1 - \mathcal{Y}_{e3}^2 - \mathcal{Y}_3^2) \sin^2(1) \quad (2.14)$$

Using (2.12) and (2.14) we now have a relation between $\sin^2(1)$ and our four \mathcal{Y}_{ij}^2 . Therefore, we can relate to our set of four \mathcal{Y}_{ij}^2 through either $\cos(1)$ or $\sin^2(1)$. Since we want ultimately information on $\cos(1)$ and there is more information through $\cos(1)$ than through $\sin^2(1)$, in what follows, we will concentrate on $\cos(1)$. We will be left with a twofold degeneracy as we will not be able to get the sign of $\cos(1)$.

On figure 1, we plot J^2 as a function of \mathcal{Y}_1^2 and \mathcal{Y}_{e3}^2 for central values of \mathcal{Y}_3^2 (0.5) and \mathcal{Y}_{e2}^2 (0.3). We see clearly that the vanishing of \mathcal{Y}_{e3}^2 leads to the vanishing of J^2 , as it must be. We also see that J^2 is a fairly linear function of \mathcal{Y}_{e3}^2 ; this is expected since the maximum value \mathcal{Y}_{e3}^2 can have is rather small compared to the other parameters and an expansion to first order in \mathcal{Y}_{e3}^2 would be adequate. For numerical purposes, we note that the largest value taken by J^2 on this figure is 2.42 10^{-3} ; it is clearly at the largest possible value of \mathcal{Y}_{e3}^2 and at $\mathcal{Y}_1^2 = 0.167$.

On figure 2, we plot curves of constant $\sin^2(1)$. When we fix \mathcal{Y}_{e2}^2 , \mathcal{Y}_3^2 , and \mathcal{Y}_{e3}^2 , if we ask what value of \mathcal{Y}_1^2 will give 25% of the maximum value that J^2 can have, we are in fact setting $\sin^2(1) = 0.25$. The straight line in the middle is the curve $\mathcal{Y}_1^2 = J_{\max}^2$ and is given by 2.7 with $\cos(1) = 0$.

III. CONSTRAINTS FROM THE \mathcal{Y}_{ij}^2 OR THEIR RATIOS

In order to be able to set some bounds on $\cos(1)$, we need at least lower limits on \mathcal{Y}_{e3}^2 and \mathcal{Y}_1^2 besides the data that we have on \mathcal{Y}_{e2}^2 and \mathcal{Y}_3^2 ; as we can see on figure

2, just an upper limit it cannot constrain $\cos(1)$. In what follows, we explore the full 4-dimensional parameter space: we allow \mathcal{Y}_1^2 to cover the whole range allowed by unitarity, and \mathcal{Y}_{e3}^2 varies from 0.001 to 0.03, since 0.03 is close to the current 3-sigma limit and 0.001 makes CP-violation extremely small at planned CP-violating experiments [12]. As for \mathcal{Y}_{e2}^2 and \mathcal{Y}_3^2 , we will work with values that can differ by 0.1 from their current central values of 0.3 and 0.5, respectively.

We assume that we have four \mathcal{Y}_{ij}^2 with their experimental uncertainties. The experimental central values of the \mathcal{Y}_{ij}^2 's (\mathcal{Y}_{ij}^2) lead to the central value of $\cos(1)$. In order to estimate the error, or range that we should associate to this central value, we use a Monte Carlo technique and we cover, for each \mathcal{Y}_{ij}^2 , the space $(\mathcal{Y}_{ij}^2 - \text{exp. error}) - (\mathcal{Y}_{ij}^2 + \text{exp. error})$. Within this 4-dimensional space, we are interested only in the largest and smallest values that $\cos(1)$ can have; these become the range that $\cos(1)$ covers with this particular combination of \mathcal{Y}_{ij}^2 and their associated errors.

As a single \mathcal{Y}_{ij}^2 , we picked \mathcal{Y}_1^2 . This choice is not unique and we could have chosen \mathcal{Y}_2^2 , or \mathcal{Y}_3^2 , or \mathcal{Y}_{e2}^2 . However, since these three parameters are linear combinations of \mathcal{Y}_1^2 and the other three \mathcal{Y}_{ij}^2 of our chosen set, we do not expect the sensitivity of $\cos(1)$ to vary much from one set to another. Therefore, we can say that \mathcal{Y}_1^2 will be representative of the limits that one will be able to set on $\cos(1)$ from the measurement of any other single \mathcal{Y}_{ij}^2 . Of course, it might be much easier to measure \mathcal{Y}_1^2 than to measure \mathcal{Y}_2^2 , for example.

We also take into consideration some ratios of \mathcal{Y}_{ij}^2 as potential fourth parameter. The first one is $\mathcal{Y}_1^2 = \mathcal{Y}_2^2 = \mathcal{Y}_3^2$ and has very similar properties to $\mathcal{Y}_2^2 = \mathcal{Y}_3^2$; the second one is $\mathcal{Y}_2^2 = \mathcal{Y}_3^2 = \mathcal{Y}_{e2}^2$ and has very similar properties to $\mathcal{Y}_2^2 = \mathcal{Y}_1^2$. We also studied $\mathcal{Y}_2^2 = \mathcal{Y}_1^2$ but it turned out to be too sensitive to both \mathcal{Y}_{e3}^2 and \mathcal{Y}_3^2 to be of any use; and similarly for $\mathcal{Y}_1^2 = \mathcal{Y}_2^2$. The same can be said of any ratio that involves \mathcal{Y}_{e1}^2 . So, we present in Tables I, and II the limits that we can set on $\cos(1)$ from measurements on \mathcal{Y}_1^2 , \mathcal{Y}_2^2 and \mathcal{Y}_3^2 . These are representative of what can be achieved. After studying the parameter space described above, we can say that:

uncertainties of 10% on the four parameters can lead to very tight bounds on $\cos(1)$; the uncertainty on \mathcal{Y}_{e3}^2 can be much larger than this without affecting the bounds very much.

An interesting constraint already occurs for the combination $(0.3, 0.5, P, \mathcal{Y}_{e3}^2)$ with a 10% uncertainty on the parameters: the first two parameters (\mathcal{Y}_{e2}^2 and \mathcal{Y}_3^2) are at their current central values while the third one (either $\mathcal{Y}_1^2 = 0.15$, $\mathcal{Y}_1^2 = 1.0$ or $\mathcal{Y}_1^2 = 2.3$) is close to the value that maximizes J^2 . We find that if \mathcal{Y}_{e3}^2 turns out to be large (0.03), then $\cos(1)$ has a range of 40-70 degrees centered at about 90 degrees, depending what P one uses; this range decreases as \mathcal{Y}_{e3}^2 increases. If the uncertainties are reduced to 5%, the range becomes 30-60 degrees and \mathcal{Y}_{e3}^2 can be reduced to 0.01.

for most combinations of ν_{e2}^2 and ν_{e3}^2 , if ν_{e1}^2 turns out to be relatively small, about 0.1, then ν_{e1}^2 has to be between 0.02 and 0.05 for any ν_{e3}^2 larger than 0.005.

the limits are not very sensitive to the uncertainty on ν_{e3}^2 ; going from 5% to 20% does not change the limits by much. If the other uncertainties are small (2%), the uncertainty on ν_{e3}^2 can go up to 50% and it is still possible to get interesting bounds on

the limits are not very sensitive to ν_{e3}^2 itself and going from 0.01 to 0.005 will not change the limits very much. When ν_{e3}^2 becomes 0.001, however, the limits are somewhat degraded but still useful.

as the value of ν_{e3}^2 becomes smaller, the uncertainties on the other parameters must decrease in order to keep interesting bounds on ; note that the uncertainty on ν_{e3}^2 can be rather large without affecting much the bounds

in general, we find that the best parameter is ν_{e1}^2 , the second best is ν_{e2}^2 and the third best is ν_{e3}^2 .

The previous analysis is very general and describes which parameters must be measured and with what accuracy in order to set limits on ν_{e3}^2 . We now turn to some potential processes that could give us the fourth information that we need in order to be able to set limits on ν_{e3}^2 .

IV. ULTRA HIGH ENERGY COSMIC RAYS

Ultra high energy cosmic rays and their detectors have attracted a fair amount of attention in recent years[13, 14, 15, 16] An interesting consequence for the UHCR neutrino spectra is due to maximal atmospheric mixings. Following maximal mixing, $\tan \theta_A = 1$ leads to a unique prediction for UHCR neutrino fluxes. It was shown that UHCR neutrinos (which are expected to be sourced by cosmic objects such as AGNs) when measured by ground based detectors, the expected flavor ratio $e : \mu : \tau = 1 : 1 : 1$ [17]. This value is also known as the standard flavor ratio and by itself constitutes an independent confirmation of the neutrino mixing data from atmospheric sources. Since we propose to extract the Dirac CP phase present in the conventional PMNS mixing matrix, our discussion will be restricted to Dirac neutrinos. Before proceeding with the analysis, let us briefly allude to the significance of this proposal. It is well known that CP violation (due to oscillation) in the leptonic mixings (even if larger than the quark sector) will nonetheless remain a hard problem to resolve[12]. This arises from the strong constraints which reactor neutrinos set on the mixing element V_{e3} [5]. As a consequence of this, even if the CP phase is large, the smallness of V_{e3} leads to phase being insensitive to any CP violating measurements.

A. The basic formalism

In the same fashion as quarks mix, massive neutrinos mix (and also oscillate) between two eigenbasis, the flavor (ν_i) and mass eigenbasis (ν_m). The two basis are related by a unitary matrix V such that $\nu_i = V \nu_m$. Here we assume the summation over the mass eigenstates. Corresponding to a particular mass eigenstate is a mass value, m_i which in the limit of small mixings determines the mixing angles. Thus, in the limit of small mixings, ν_m mixes eigenstates ν_1 and ν_2 , while ν_i mixes eigenstates ν_2 and ν_3 and ν_m mixes the eigenstates ν_1 and ν_3 .

In the context of UHCR neutrinos which travel astronomical distances, the coherence between the various mass eigenstates is averaged out. In other words, after production these neutrinos essentially travel as individual mass eigenstate. At the point of detection, they are in the flavor states. Therefore, the detection probability in a given flavor eigenstate is

$$\begin{aligned} e &= 1 + 2x(2c_A^2 - 1) ; x = (s_A c_A)^2 ; \\ &= 2x c_A^2 + 2(c_A^4(1 - 2x) + s_A^4) ; \\ &= s_A^2 + 2x s_A^2(1 - c_A^2) ; \end{aligned} \quad (4.15)$$

where s and c denote sine and cosine, respectively. From the above expressions and the experimental fact $\theta_A = 45^\circ$, it follows that all neutrino flavors must be detected with the same weight factor. In deriving this result, we have disregarded the mixing corresponding to reactor experiments, which is consistent with zero [5]. This result is also independent of the solar angle θ_S .

B. Neutrino Fluxes and ν_{ij}^2

Let us revise in more detail the arguments from the previous section. Consider the probability of oscillating from flavor to

$$\begin{aligned} P &= \sum_{i=1}^3 \sum_{j=1}^3 \text{Re}[\mathcal{K}_{ij}] \sin^2(\theta_{ij}) \\ &+ \sum_{i=1}^3 \sum_{j=1}^3 \text{Im}[\mathcal{K}_{ij}] \sin(\theta_{ij}) \cos(\theta_{ij}) ; \\ \mathcal{K}_{ij} &= V_{i1} V_{i2} V_{j1} V_{j2} ; \quad \theta_{ij} = \frac{m_i^2 - m_j^2}{L=4E} : \end{aligned} \quad (4.16)$$

We can express the real and imaginary parts of \mathcal{K}_{ij} in terms of moduli as follows:

$$\begin{aligned} 2\text{Re}[\mathcal{K}_{ij}] &= \sum_{jk} \nu_{ij}^2 \nu_{jk}^2 + \nu_{ij}^2 \nu_{jk}^2 \\ &\quad - c_{ijk} \nu_{ik}^2 \end{aligned} \quad (4.17)$$

and

$$\text{Im}[\mathcal{K}_{ij}] = J''_{ij} \quad (4.18)$$

where we have defined:

$$\begin{aligned} C_{ijk} &= 1 \text{ if } i \neq j; j \neq k; k \neq i \\ &= 0 \text{ otherwise} \end{aligned} \quad (4.19)$$

and ϵ as the antisymmetric tensor

$$\epsilon = \begin{matrix} 0 & 1 & 1 \\ 1 & 0 & 1 \\ 1 & 1 & 0 \end{matrix} \quad (4.20)$$

We are interested here only in the probabilities for ν_1 , ν_2 , ν_e and $\bar{\nu}_e$. After combining two terms ($\nu_{13} = \nu_{23}$ to high accuracy), expressing the third term as a combination of ν_{ij}^2 and averaging over the oscillating terms, we obtain

$$\begin{aligned} P &= 2\nu_3^2\nu_3^2 (\nu_{e1}^2\nu_{e2}^2 - \nu_1^2\nu_2^2) \\ &\quad - \nu_1^2\nu_2^2) ; \\ P_e &= 2\nu_{e3}^2\nu_3^2 (\nu_1^2\nu_2^2 - \nu_{e1}^2\nu_{e2}^2) \\ &\quad - \nu_1^2\nu_2^2) ; \\ \bar{P}_e &= 2\nu_3^2\nu_{e3}^2 (\nu_1^2\nu_2^2 - \nu_{e1}^2\nu_{e2}^2) \\ &\quad - \nu_1^2\nu_2^2) ; \end{aligned} \quad (4.21)$$

One then uses the relations

$$\begin{aligned} \nu_{e1}^2 &= 1 - \nu_{e2}^2 - \nu_{e3}^2 ; \\ \nu_2^2 &= 1 - \nu_1^2 - \nu_3^2 ; \\ \nu_1^2 &= \nu_{e2}^2 + \nu_{e3}^2 - \nu_3^2 ; \\ \nu_3^2 &= \nu_1^2 + \nu_2^2 - \nu_{e2}^2 ; \end{aligned} \quad (4.22)$$

to express these probabilities in terms of our four ν_{ij}^2 .

Note that when averaging over the oscillating terms, the third term of 4.16 vanishes; therefore, one will not be able to observe directly CP-violation with UHCR's.

If we assume that the main production mode of these UHCR is [18]

$$p + \bar{\nu}_e + X ; \quad (4.23)$$

with subsequent decay of the $\bar{\nu}_e$ into muons, electrons, and neutrinos, we conclude that there will be two (or $\bar{\nu}_e$) for every ν_e (or $\bar{\nu}_e$) and virtually no ν_e (or $\bar{\nu}_e$). The initial fluxes are then $\nu_{e1}^0 = 2\nu_{e2}^0$, and $\nu_{e3}^0 = 0$. In order to calculate a given neutrino flux that reaches the earth, we take into account the probability that this neutrino will oscillate into other types of neutrinos and the probabilities that other neutrinos will oscillate into this type of neutrino. Up to a common geometrical factor, the observed terrestrial fluxes are:

$$\begin{aligned} \nu_{e1}^t &= \nu_{e1}^0 (1 + P_e - P_{\bar{e}}) ; \\ \nu_{e2}^t &= \nu_{e2}^0 (2P_e - 2P_{\bar{e}}) ; \\ \nu_{e3}^t &= \nu_{e3}^0 (2P_{\bar{e}} + P_e) ; \end{aligned} \quad (4.24)$$

In terms of matrix elements, we get

$$\begin{aligned} \nu_{e1}^t &= \nu_{e1}^0 (1 - 2\nu_{e2}^2 (\nu_3^2 - \nu_{e2}^2) \\ &\quad + 2\nu_1^2 (\nu_1^2 - 2\nu_{e2}^2)) \\ &\quad - 2\nu_{e3}^2 (\nu_1^2 + 2\nu_{e2}^2 - \nu_3^2) + 2\nu_{e3}^4) ; \\ \nu_{e2}^t &= \nu_{e2}^0 (2 + (\nu_1^2 - \nu_3^2) (\nu_{e2}^2 - 4\nu_3^2) \\ &\quad - \nu_1^2 (\nu_3^2 + 2\nu_{e2}^2 - 4\nu_3^2) - 4\nu_1^2) \\ &\quad + \nu_{e3}^2 (\nu_3^2 - \nu_1^2) ; \\ \nu_{e3}^t &= \nu_{e3}^0 (4\nu_3^2 (\nu_1^2 - \nu_3^2) - \nu_{e2}^2 (\nu_1^2 - \nu_{e2}^2) \\ &\quad + 3\nu_{e2}^2 (\nu_3^2 - \nu_{e2}^2) \\ &\quad + \nu_{e3}^2 (2 + 3\nu_1^2 - 3\nu_3^2 - 2\nu_{e2}^2 - 2\nu_{e3}^2) \\ &\quad + \nu_1^2 (1 - 4\nu_1^2 - 4\nu_3^2 + 6\nu_{e2}^2)) \end{aligned} \quad (4.25)$$

Clearly, we don't know the original neutrino fluxes at the source. Therefore, it is more meaningful to try to measure ratios of neutrino fluxes. We will consider the ratios $R_e = \frac{\nu_{e1}^t}{\nu_{e1}^0} = \frac{\nu_{e2}^t}{\nu_{e2}^0}$ and $\bar{R}_e = \frac{\nu_{e3}^t}{\nu_{e3}^0} = \frac{\bar{\nu}_{e3}^t}{\bar{\nu}_{e3}^0}$ and calculate how they vary when we cover the parameter space available. Our results are summarized in Table III. One can see that:

by numerical accident, ν_3^2 close to 0.5 has a very strong influence on R_e and \bar{R}_e and tends to keep them close to 1

if ν_3^2 stays close 0.5 to within 10%, R_e and \bar{R}_e remain close to 1, for any value of ν_{e2}^2 and ν_{e3}^2 that are within the experimentally allowed ranges

when one varies ν_3^2 by 20%, either up or down, it is possible for R_e and \bar{R}_e to differ from 1 by as much as 20%. Unfortunately, these large discrepancies require values of ν_1^2 such that $\nu_1^2 \approx 0$ or $\nu_1^2 \approx 1$, which means very little CP-violation

ν_{e3}^2 has very little impact and varying it from 0.01 to 0.005 will change R_e and \bar{R}_e , typically by 1% or so.

Therefore, we can say that even within the standard production mechanism for the UHCR, deviations of R_e and \bar{R}_e by 20% from their expectation value of 1 are possible with the current experimental data but require in general pushing these data to their limits and CP-violation to be vanishingly small.

C. Neutrino Fluxes and

In order to study the bounds one could set on ν_1^2 if one were to measure R_e with a given accuracy, we express ν_1^2 in terms of R_e and use that result directly into our expression of $\cos(\theta)$ (2.10). Again, we use a Monte Carlo technique to scan the allowed parameter space. As a technical detail, we note that we have a quadratic equation to solve with two possible values for ν_1^2 but only one value respects unitarity and leads to a positive value of J^2 ; events that do not respect unitarity are excluded from our Monte Carlo. In Table IV, we

summarise our results. We see that:

the most important parameters are \mathcal{Y}_3^2 and R_e , where the uncertainties must be rather small, while \mathcal{Y}_{e2}^2 and \mathcal{Y}_{e3}^2 can tolerate much larger errors without degrading the limits much.

In general, a precision of two percent on all 4 parameters leads to tight constraints on \mathcal{Y}_{e3}^2 ; this can be relaxed to 10% for \mathcal{Y}_{e2}^2 and up to 25% for \mathcal{Y}_{e3}^2 without losing much on the bounds on

large or small values of R_e (1.13 or 0.84, for example) require higher precision in the four parameters in order to keep $\cos(\phi)$ away from +1 or -1; the precision required on \mathcal{Y}_{e2}^2 and \mathcal{Y}_{e3}^2 is still lower than that on the other two parameters. Recall that $\cos(\phi) = 1$ means no CP-violation.

As \mathcal{Y}_{e3}^2 gets smaller, a higher precision on the parameters is necessary in order to keep the same tight range on

With some combinations of parameters, it is possible to exclude $\phi = 0$ with a precision of a few percent on the parameters

An uncertainty of 5% on R_e can limit it to a 90-degree range or smaller with certain combination of parameters

The precision required in order to get interesting constraints on ϕ is daunting but this was expected since we saw that \mathcal{Y}_1^2 was the least sensitive of our three parameters to set limits on ϕ .

V. NEW PHYSICS AND

This general behaviour of cosmological neutrino fluxes has been noted before [17] and comes directly from the fact that \mathcal{Y}_3^2 is close to 0.5. As \mathcal{Y}_3^2 goes away from 0.5, (current data allow a deviation of up to 20%) the ratios can differ substantially from 1:1:1, as we just saw. This brings the question of how one would interpret ratios that would differ much more than 8%, say 30% or more. It would be difficult to explain these anomalies within the SM and such discrepancies might suggest some new physics. This new physics could bring its own CP-violation, which could be a la Dirac; we would then deal with an effective CP-phase such that $\phi_{\text{effective}} = \phi + \phi_{\text{new}}$.

We will consider new physics beyond massive neutrinos and for illustration purposes, we choose non-radiative neutrino decays.

A. Non-radiative neutrino decays and ϕ_{eff}

The notion of non-radiative neutrino decay as a source of deviations from the standard ratio was first discussed in [19] and we refer to this paper for details. Essentially, in this model, the observable flavor ratio is modified to be

$$e : : = \mathcal{Y}_{e1}^2 : \mathcal{Y}_1^2 : \mathcal{Y}_{e3}^2 ; \quad (5.26)$$

where we assume normal mass hierarchy.

Contrary to the SM flux ratios, the ratio $R_e = \mathcal{Y}_{e3}^2 / \mathcal{Y}_{e1}^2$ is a direct measure of

$$R_e = \frac{\mathcal{Y}_{e3}^2}{\mathcal{Y}_{e1}^2} : \quad (5.27)$$

which proved to be the best variable to set constraints on ϕ . Table V shows what kind of limit one could obtain with such a scenario. We note that:

uncertainties in the 5% - 10% range can lead to interesting constraints on ϕ_{eff} :

The limits are insensitive to the uncertainty on \mathcal{Y}_{e3}^2 .

In this model, flux ratios of up to 3 are allowed with current data. This limit depends on \mathcal{Y}_{e3}^2 and as \mathcal{Y}_{e3}^2 decreases, so does the upper limit of the ratio

V I. CONCLUSIONS

In this paper we have shown how it is possible to get information about CP-violation in the leptonic sector without performing any direct experiment on CP-violation. In the usual parametrization of the leptonic mixing, the mixings are described by three mixing angles and the fourth parameter is the CP-violating phase, ϕ . All the information about mixing and CP-violation can also be described completely by four mixing elements, four \mathcal{Y}_{ij}^2 . We have shown how one can extract information on $\sin^2(\phi)$ and $\cos(\phi)$ from four \mathcal{Y}_{ij}^2 or three \mathcal{Y}_{ij}^2 and a ratio of two \mathcal{Y}_{ij}^2 . We used two such ratios: $R_e = \mathcal{Y}_{e3}^2 / \mathcal{Y}_{e1}^2$ and $R_{\nu} = \mathcal{Y}_{e2}^2 / \mathcal{Y}_{e1}^2$.

As a first constraint that does not require particularly precise data, we find that if \mathcal{Y}_{e3}^2 were larger than $\mathcal{Y}_{e1}^2 = \mathcal{Y}_{e2}^2 = \mathcal{Y}_{\text{max}}^2$, then ϕ would have to be in the first or fourth quadrant.

In general, when the four parameters have uncertainties of 10%, it is possible to get interesting constraints on ϕ on some of the parameter space. For example, assuming 10% errors, if \mathcal{Y}_{e2}^2 and \mathcal{Y}_{e3}^2 keep their current experimental central values and \mathcal{Y}_{e1}^2 turns out to be about 0.15, then ϕ has a 70 degree range centered at about 90 degrees if \mathcal{Y}_{e3}^2 turns out to be 0.03; this range decreases to about 40 degrees if one measures R_e and it decreases as \mathcal{Y}_{e3}^2 increases. If the uncertainties are reduced to 5%, then the ranges on ϕ become 30-60 degrees and can tolerate a value of 0.01 for \mathcal{Y}_{e3}^2 . We also found that, for most combinations of \mathcal{Y}_{e2}^2 and \mathcal{Y}_{e3}^2 , a small value of \mathcal{Y}_{e1}^2 (0.1) implies that ϕ is between $\phi = 2$ and

It turns out that $\cos(\phi)$ is not particularly sensitive to \mathcal{Y}_{e3}^2 over most of the parameter space. This implies that once the errors are reduced to the 2% level, even if the error on \mathcal{Y}_{e3}^2 stayed at 10%, it would not degrade the constraints on ϕ by much. Of the three variables investigated here, the best one turned out to be R_e .

In order to get the fourth piece of information needed to set bounds on ϕ , we explored the use of ultra high energy cosmological neutrinos. Generally, due to a numerical accident stemming mostly from $\mathcal{Y}_{e3}^2 = 0.5$, the cosmological

neutrino fluxes are very similar once they reach the earth. However, current data allow cosmic neutrino fluxes to differ from their central, expected value of 1 by up to 20% : this requires pushing the parameters to the acceptable limits and implies that CP violation in the leptonic sector is vanishingly small. Unfortunately, the uncertainties on the data would have to be at the few percent level on the cosmic neutrino fluxes and on $\bar{\nu}_{e2}$ in order to set interesting limits on θ . Finally, we studied a non-radiative decay model of neutrinos that could lead to flux ratios

very different from 1. Indeed, in this model, the current data allow for neutrino fluxes to differ by a factor of up to three. Fortunately, in this model, one ratio of neutrino fluxes is θ and leads to rather interesting constraints on θ with experimental uncertainties of 10% on ratios of cosmic neutrino fluxes.

Acknowledgements: We wish to thank Dr. Irina Mocioiu for useful comments. This work is funded by NSERC (Canada) and by the Fonds de Recherche sur la Nature et les Technologies du Québec.

[1] SuperKamiokande Collaboration, Y. Fukuda, Phys. Rev. Lett. 81, 1562 (1998); GALLEX Collaboration, W. Hampel et al, Phys. Lett. B 447, 127 (1999); SAGE Collaboration, J. N. Abdurashitov et al. Phys. Rev. C 60, 055801 (1999); Homestake Collaboration, B.T. Cleveland et al, Astrophys. J. 496 505 (1998); GNO Collaboration, M. Altmann et al., Phys. Lett. B 490 16 (2000); SNO Collaboration, Q.R. Ahmad et al, Phys. Rev. Lett. 87, 071301 (2001); S. Fukuda et al, SuperKamiokande Collaboration, Phys.Lett. B 539, 197 (2002); S.N. Ahmed et al., SNO Collaboration, arXiv:nucl-ex/0309004; SuperKamiokande Collaboration, Y. Ashie et al., hep-ex/0404034.

[2] B. Pontecarvo, J. Exptl Theoret. Phys. 33, 549 (1957) [Sovt. Phys. JETP 6, 429 (1958)] J. Exptl. Theoret. Phys. 34, 247 (1957) [Sovt. Phys. JETP 7, 172 (1958)]

[3] M. Maltoni, T. Schwetz, M.A. Tortola, J.W.F. Valle, hep-ph/0405172.

[4] J. Arafune, J. Sato, Phys. Rev. D 55, 1653-1658 (1997); J. Arafune, M. Koide, J. Sato, Phys. Rev. D 56, 3093-3099 (1997) and erratum *ibid.* D 60 (1999) 119905; H. Minakata, H. Nunokawa, Phys. Lett. B 413, 369-377 (1997); H. Minakata, H. Sugiyama, Phys. Lett. B 580 (2004) 216-228; K. Hiraide et al, hep-ph-0601258; K. Kimura, A. Takamura, T. Yoshikawa, hep-ph-0603141; F.R. Linkhamer hep-ph-0601116; H. Minakata hep-ph-0604088;

[5] The CHOOZ collaboration, M. Apollonio et al., Phys. Lett. B 466, 415 (1999); F. Boehm et al, Phys. Rev. Lett. 84, 3764 (2000); Phenomenological implications for CHOOZ data on active three flavor oscillations was first examined by Mohan Natayan, G. Rajasekaran, S. Uma Sankar, Phys. Rev. D 58, 031301 (1998).

[6] See for example M. Divali, et al., Very Long Baseline Neutrino Oscillation Experiment for Precise Determination of Oscillation Parameters in Search for θ_{13} , θ_{23} , Appearance and CP-Violation, hep-ex-0211001

[7] Z. Maki, M. Nakagawa, S. Sakata, Prog. Theor. Phys. 28, 870 (1962)

[8] We could also use supernova neutrino data as additional observable, but, given the possibility of detecting UHCR neutrinos more frequently than a supernova burst, we shall not consider this option.

[9] C. Hamzaoui, Phys. Rev. Lett. 61, 35 (1988); C. Hamzaoui, Geometrical Parameterization of the Quark Mixing Matrix, in Rare Decay Symposium, Proceedings, Vancouver, Canada, November 1988; D. Baryan, J.N. Ng, R. Numao, J.-M. Poutissou, Edts., p. 469; A. Campana, C. Hamzaoui, V. Raha, Phys. Rev. D 39, 3435 (1989)

[10] C. Jarlskog, Phys. Rev. Lett. 55, 1039 (1985); D. Dunietz, O. Greenberg, D. D. Wuest, Phys. Rev. Lett. 55, 2935 (1985)

[11] See for example: R.H. Mohapatra, et al., hep-ph-0510210; M.C.Gonzalez-Garcia, Y. Nir, Rev. Mod. Phys. 75, (2003) 345-4002

[12] S. Petcov, in Neutrino 2004, Eds. J. Dumarchez, Th. Patzi, F. Vannucci; Nucl. Phys. (Proc. Suppl.) 143 (2005) p. 159; O. Mena, S. Palomares-Ruiz, S. Pascoli, Phys. Rev. D 73 (2006) 073007; O. Mena, Mod. Phys. Lett. A 20, (2005) 1-17.

[13] J.F. Beacom, N.F. Bell, D. Hooper, J.G. Learned, S. Pakvasa, T.J.W. Eiler, Phys. Rev. Lett. 92, 011101 (2004); P. Keranen, J.M. Aalampi, M. Myyryläinen, J.R. Iittinen, Phys. Lett. B 574, 162 (2003).

[14] J. Ahrens et al., IceCube Collaboration, Astrophys. J. 620, 507 (2004); Teresa Montaruli et al., ANTARES Collaboration, proceedings of 28th International Cosmic Ray Conferences (ICRC 2003), Tsukuba, Japan, 31 Jul - 7 Aug 2003, arXiv:physics/0306057; S.E. Tzanarias (for the collaboration), NESTOR Collaboration, Nucl. Instrum. Meth. A 502, 150 (2003); M. Takeda et al., Astrophys. J. 522, 225 (1999); D.J. Bird et al., HIRÉS, Astrophys. J. 424, 491 (1994).

[15] A. Osipowicz et al., KATRIN Collaboration, hep-ex/0109033; H. Paes, Thomas J.W. Eiler, Phys. Rev. D 63, 113015 (2001).

[16] J. Jones, I. Mocioiu, I. Sarcevic, M.H. Reno, Int. J. Mod. Phys. A 20 (2005) p. 1204-1211; P.D. Serpico, M. Kachelrieß, Phys. Rev. Lett. 94 (2005) 211102; P.D. Serpico, Phys. Rev. D 73 (2006) 047301; W.W. Winter, hep-ph-0604191

[17] H. Athar, M. Jezabek, O. Yasuda, Phys. Rev. D 62, 103007 (2000); Luis Bento, Petteri Keranen, Jukka M. Aalampi, Phys. Lett. B 476, 205 (2000).

[18] Other production mechanisms can affect the fluxes seen on earth. See, for example J. Jones, I. Mocioiu, M.H. Reno, I. Sarcevic, Phys. Rev. D 69 (2004) 033004

[19] J.F. Beacom, N.F. Bell, D. Hooper, S. Pakvasa, T.J. W. Eiler, Phys. Rev. Lett. 90 181301, (2003).

Figure Captions

Figure 1

J^2 as a function of \mathcal{V}_{e3}^2 and \mathcal{V}_1^2 for the current central values of \mathcal{V}_{e2}^2 (0.3) and \mathcal{V}_3^2 (0.5)

Figure 2

Different values of $\sin^2(\theta)$ in the $\mathcal{V}_{e3}^2 - \mathcal{V}_1^2$

plane. From the outside, inward, we plot $\sin^2(\theta) = 0; 0.1; 0.25; 0.5; 0.75; 0.95; 1$. The line in the middle corresponds to $\sin^2(\theta) = 1$ and is given by eq. 2.7 with $\cos(\theta) = 0$; the most outward curves correspond to $\cos(\theta) = 1$.